Correlations of πN partial waves for multireaction analyses

M. Döring,[1,2,*] J. Revier,[3] D. Rönchen,[4] and R. L. Workman[5,†]

[1]*Institute for Nuclear Studies; Astronomy, Physics, and Statistics Institute of Sciences; Department of Physics, George Washington University, 725 21st Street, NW, Washington, DC 20052, USA*

[2]*Thomas Jefferson National Accelerator Facility, 12000 Jefferson Avenue, Newport News, Virginia 23606, USA*

[3]*Department of Physics, George Washington University, 725 21st Street, NW, Washington, DC 20052, USA*

[4]*Helmholtz-Institut für Strahlen- und Kernphysik (Theorie) and Bethe Center for Theoretical Physics, Universität Bonn, 53115 Bonn, Germany*

[5]*Institute for Nuclear Studies and Department of Physics, George Washington University, 20101 Academic Way, Ashburn, Virginia 20147, USA*

(Received 7 April 2016; revised manuscript received 11 May 2016; published 15 June 2016)

In the search for missing baryonic resonances, many analyses include data from a variety of pion- and photon-induced reactions. For elastic πN scattering, however, usually the partial waves of the SAID (Scattering Analysis Interactive Database) or other groups are fitted, instead of data. We provide the partial-wave covariance matrices needed to perform correlated χ^2 fits, in which the obtained χ^2 equals the actual χ^2 up to nonlinear and normalization corrections. For any analysis relying on partial waves extracted from elastic pion scattering, this is a prerequisite to assess the significance of resonance signals and to assign any uncertainty on results. The influence of systematic errors is also considered.

DOI: 10.1103/PhysRevC.93.065205

I. INTRODUCTION AND MOTIVATION

The existence and properties [1] of most N and Δ resonances have been determined through elaborate analyses [2–9] of πN elastic scattering data. More recently, however, baryon spectroscopy has been driven by the progress made in the measurement and analysis of meson photoproduction reactions. These analyses often take a multichannel approach, incorporating reactions with a variety of initial (πN, γN) and final (πN, ηN, $K\Lambda$, $K\Sigma$, ωN, $\pi\pi N$) states.

In order to build on the progress made in the earlier πN elastic analyses, multichannel analyses [10–22] have usually fitted πN amplitudes, derived from previous studies [2–9], together with reaction data. The fitted amplitude pseudodata have either been taken from single-energy analyses (SE) or energy-dependent (ED) fits covering the resonance region. The SE analysis amplitudes, derived from fits to narrow energy bins of data, have associated errors which have been used in the multichannel fits or enlarged when these fits have become problematic. The smoother ED amplitudes have also been taken at discrete energies, typically with subjective errors not derived from the fit to data.

There are several problems associated with fits to amplitude pseudodata, which we have attempted to address in this work. The most obvious of these is the fact that the goodness of fit to these sets of amplitudes cannot be translated into a quality of fit to the underlying dataset. The subsequent comparison to experimental πN data may result [23] in poorer than expected agreement. In addition, uncertainties on the SE amplitudes [2–5] do not account for correlated errors, which can be substantial in some cases.

In baryon spectroscopy, based on multireaction analysis, this has unwanted side effects. First, a statistical analysis of fit results is difficult if one of the input channels is not given by data. Second, as a consequence, the significance of resonance signals, detected in such multireaction fits, is difficult to quantify. Consider, for example, the situation in which an additional resonance term leads to considerable improvement in the description of kaon photoproduction data. The description in the $\pi N \to \pi N$ reaction might then barely change. Indeed, one of the main motivations for the baryon photoproduction program is to search for missing states with small πN resonance couplings. Yet, there will be a nonzero impact in the description of the $\pi N \to \pi N$ reaction. As long as that small change in χ^2 cannot be tested in terms of statistical criteria, based on πN data, the significance of the proposed new state will be difficult to assess.

In a similar way, chiral perturbation theory (CHPT) and its unitary extension (UCHPT) may profit from an improved representation of SE amplitudes. The relevance of elastic πN scattering partial waves for chiral dynamics, to study the $\pi N \sigma$ term or isospin breaking, or to obtain a quantitative measure of low-energy constant (LEC) uncertainties, is reflected in the literature [24–38]. Recently, several groups have begun to fit low-energy πN data directly [39,40].

In UCHPT, the focus lies less on spectroscopy than on the understanding of resonance dynamics and its nature in terms of hadronic components. Usually, the S-wave amplitudes S_{11} and S_{31} are subjects of interest. For example, in Ref. [41] the S_{11} and S_{31} partial waves were fitted up to the energy of the $N(1535)S11$ resonance and the $N(1650)S11$ emerged. Furthermore, with the same hadronic amplitude, pion and η photoproduction could be predicted [42,43]. The role of chiral dynamics in S-wave baryonic resonances, including fits to πN partial waves, has been studied by many groups [44–53]. Other examples, in which fits to πN partial waves are crucial to investigate chiral dynamics and to test models, include the

*doring@gwu.edu

†rworkman@gwu.edu; SAID web page: http://gwdac.phys.gwu.edu/

D_{33} partial wave [54–57] and a family of $J^P = 1/2^-, 3/2^-$ states [52,53,58]. Clearly, an improved representation of πN data beyond SE amplitudes will lead to a more reliable determination of LECs, and thus, to more reliable predictions of other hadronic reactions within UCHPT.

In summary, SE πN amplitudes represent the test ground for a wide range of theory and models from baryon spectroscopy and chiral resonance dynamics to tests of quark models [59–61]. Attaching more statistical meaning to those solutions would considerably advance the understanding of hadron dynamics.

The aim of this paper is to provide an easy-to-implement representation of the $\pi N \to \pi N$ data in terms of covariance matrices and best χ^2 values for each set of SE amplitudes. With this, the $\pi N \to \pi N$ reaction can be included in multireaction spectroscopy fits in a statistically more meaningful way through correlated χ^2 fits. The effect of systematic errors associated with the underlying data provides a subtle difficulty which we discuss in detail below.

Together with this study, numerical values for matrices and χ^2 values are provided on the Scattering Analysis Interactive Database (SAID) [62] and JPAC [63] web pages for further use.

II. GENERATING SE AMPLITUDES

In the following, we restrict our attention to the single-energy (SE) amplitudes, which are generated starting from a global, energy-dependent (ED) fit, and give a better fit to data. These amplitudes show more scatter than would appear in the ED fit. This is preferable in a multichannel analysis which may interpret apparently random fluctuations in the single-channel fit as resonance signatures. Here, we use the most recent ED fit of Ref. [2].

Data for each of the SE analyses have been taken from the SAID database [62] with an energy interval depending on the density of experimental measurements. This interval varies from 2 MeV, for the low-energy region, to 50 MeV, at the highest energies where data are sparse. A finite binning in energy increases the number of data constraints but requires an assumption for the energy dependence, which is taken to be linear. The quoted amplitudes correspond to the central energy. The χ^2 fit to data is carried out, using the form

$$\chi^2 = \sum_i \left(\frac{N\Theta_i - \Theta_i^{\rm exp}}{\epsilon_i} \right)^2 + \left(\frac{N-1}{\epsilon_N} \right)^2, \qquad (1)$$

where $\Theta_i^{\rm exp}$ is an experimental point in an angular distribution and Θ_i is the fit value. Here the overall systematic error, ϵ_N, is used to weight an additional χ^2 penalty term due to renormalizaton of the fit by the factor N. The statistical error is given by ϵ_i. It has been shown that the above renormalization factors can be determined at each search step and do not have to be explicitly included in the search [64]. Empirical renormalization factors have also been used in fits to low-energy data based on chiral perturbation theory [40].

The search is stabilized in two ways. Clearly, one cannot search an infinite number of partial waves. As a result, the number of included waves is determined by their contribution to the cross section, with all higher waves being taken from the ED fit. In addition, ED amplitude pseudodata are included in the fit, with large uncertainties, to keep the SE solution in the neighborhood of the ED result. Clearly, with overly tight constraints, one could generate an SE fit arbitrarily close to the ED value. However, in practice, the constraints allow sufficient freedom and contribute very little (less than 1%) to the total χ^2. The searched waves are elastic until their contribution to the reaction cross section is significant, as determined in the ED analysis.

III. USING THE ERROR MATRIX

A pion-nucleon partial wave f_i is parametrized by two real parameters. Here, we choose the phase shift δ_i and ρ_i, where

$$\cos\rho_i = \eta_i, \qquad (2)$$

with elasticity parameter η_i and the scattering amplitude

$$\begin{aligned} \mathrm{Re}\, f_i &= \tfrac{1}{2}\cos\rho_i \sin(2\delta_i), \\ \mathrm{Im}\, f_i &= \tfrac{1}{2}[1 - \cos\rho_i \cos(2\delta_i)]. \end{aligned} \qquad (3)$$

In the following, the set of parameters for a given set of partial waves is called generically A_i, ordered in a vector $\mathbf{A}$. The χ^2 of a SE solution can be expanded around the minimum at $\mathbf{A} = \hat{\mathbf{A}}$,

$$\chi^2(\mathbf{A}) = \chi^2(\hat{\mathbf{A}}) + (\mathbf{A} - \hat{\mathbf{A}})^T \hat{\Sigma}^{-1} (\mathbf{A} - \hat{\mathbf{A}}) + \mathcal{O}(\mathbf{A} - \hat{\mathbf{A}})^3, \qquad (4)$$

where $\hat{\mathbf{A}}$ is the estimate of the partial waves from data and $\hat{\Sigma}$ is the estimate of the covariance matrix. A *correlated* χ^2 *fit* to a SE solution means the use of the same Eq. (4) for the χ^2 up to $\mathcal{O}(\mathbf{A}^2)$, in particular of the full covariance matrix and not only its diagonal elements given by the partial-wave variances $(\Delta A_i)^2$. Thus, using $\hat{\Sigma}$ and $\chi^2(\hat{\mathbf{A}})$ of this paper in a correlated χ^2 fit provides in principle the same χ^2 as fitting to the actual data up to $\mathcal{O}(\mathbf{A}^2)$, resolving the issues raised in the introduction.

In an actual correlated χ^2 fit, either (δ_i, ρ_i) may be fitted, using the quoted covariance matrices, or, the possibly more familiar scattering amplitudes (Re f_i,Im f_i) may be utilized, requiring a transformation of the covariance matrices,

$$\hat{\Sigma}_f = Q^T \hat{\Sigma} Q, \qquad (5)$$

where Q is a block-diagonal matrix $Q = \mathrm{diag}(Q_j)$ with

$$Q_j = \begin{pmatrix} \cos\rho_i \cos(2\delta_i) & \cos\rho_i \sin(2\delta_i) \\ -\frac{1}{2}\sin\rho_i \sin(2\delta_i) & \frac{1}{2}\sin\rho_i \cos(2\delta_i) \end{pmatrix}, \qquad (6)$$

for inelastic partial waves, with $\rho_i \neq 0$, and

$$Q_j = (\cos(2\delta_i)\ \sin(2\delta)), \qquad (7)$$

for the elastic partial waves (note that Q is not necessarily a square matrix). For groups accustomed to fitting the amplitudes f_i, it may be more convenient in practice to evaluate (δ_i, ρ_i) using Eq. (2) and inverting Eqs. (3) to fit to the quoted covariance matrices directly.

A. Format of covariance matrices

The format of covariance matrices $\hat{\Sigma}$ and χ^2 estimates $\chi^2(\hat{\mathbf{A}})$ are specified on the SAID web page [62]. At the time

of publication, we quote the parameters corresponding to the WI08 solution [2]. The web page will be updated as new data are produced and analyzed. Along with the necessary parameters to carry out correlated χ^2 fits, simple subroutines are provided to read the parameters into suitable variables. The parameters to describe the χ^2 are central W of the energy bin of a given SE solution, ordering of partial wave δ_i and ρ_i parameters according to isospin I, orbital angular momentum L, total angular momentum J, and the actual values of $\hat{\mathbf{A}}$, $\chi^2(\hat{\mathbf{A}})$ and $\hat{\Sigma}$, in the given ordering. Additionally, the number of data points in the bin is quoted.

B. Representation of the χ^2

As discussed, $\hat{\mathbf{A}}$, $\chi^2(\hat{\mathbf{A}})$, and $\hat{\Sigma}$ for SE solutions provide the necessary input for other groups to carry out fits with a χ^2 that represents, in principle, the χ^2 of a direct fit to πN data. A few remarks concerning the advantages and limitations of this method are in order.

(1) Nonlinear contributions. As discussed following Eq. (4), a correlated χ^2 fit captures only the quadratic terms in the expansion around the minimum. Nonlinear corrections of $\mathcal{O}(\mathbf{A}^3)$ are neglected. Testing selected covariance matrices, we found that nonlinear corrections only become relevant far beyond the parameter region over which a fit is considered to be good. In Sec. IV an explicit example is discussed.

(2) Finite bin width. As mentioned, the bin widths become up to 50 MeV wide at the largest energies. However, partial-wave solutions have a smooth energy dependence, and single-energy solutions are allowed to vary linearly within a bin. The impact on the χ^2 from the finite bin width is not significant and only central values of the bins are quoted.

(3) Electromagnetic corrections. As the SE solutions are corrected using the method described in detail in Ref. [5], other groups using the present results do not have to implement electromagnetic corrections required to fit the data. Conversely, the implementation of electromagnetic corrections cannot be altered without a refit to the data.

(4) Renormalization. The SE solutions are obtained by allowing for a multiplicative renormalization according to Eq. (1). Any group using the present results implicitly accepts the normalization obtained in the SAID analysis of elastic πN scattering. Beyond this, no additional renormalization can be performed in correlated χ^2 fits. The effect of renormalization becomes increasingly relevant when moving away from the estimated χ^2 minimum at $\mathbf{A} = \hat{\mathbf{A}}$. We discuss a typical example in Sec. IV.

The effect from renormalizations seemingly frozen at the SAID SE solution value at $\mathbf{A} = \hat{\mathbf{A}}$ represents the largest difference between the correlated and the actual χ^2, in which renormalization is dynamically adapted for any $\mathbf{A}$. Yet, as renormalization tends to be small to moderate, and for $\mathbf{A}$ in the vicinity of $\hat{\mathbf{A}}$, the effect can be neglected.

In summary, there are advantages in using the present fit method over a direct fit to data (no need to implement electromagnetic corrections), but also limitations. Especially if a correlated χ^2 fit is poor, i.e., with parameters $\mathbf{A}$ far away from $\hat{\mathbf{A}}$, the correlated and actual χ^2 can be quite different. In that case, one can only resort to a direct fit to data, allowing for dynamic renormalization. Then, the fit function must be renormalized, rather than the data, to avoid the bias discussed in Ref. [65]. See also Ref. [66] for a further discussion of the topic.

With the limitations discussed, correlated χ^2 fits still represent a much improved treatment of the elastic πN reaction, compared to uncorrelated fits to SE solutions, as available up to now. This will be demonstrated in an example in the next section.

IV. AN EXPLICIT EXAMPLE

Table I compares fits to data with laboratory pion kinetic energies T_π between 87 and 92 MeV. Quoted are the phase shifts $\hat{A}_i = \hat{\delta}_i$(deg). The fit WI08 [2] is an ED parametrization of data covering the full resonance region (second column). It employs a normalization of the fit function. Smaller partial waves, present in the ED solution but not searched in the SE fit, are omitted from the table.

From this starting point, the most important partial waves have been searched to fit data in the chosen energy bin. In this case, S_{11}, S_{31}, P_{11}, and P_{33} phase shifts have been searched with other parameters held fixed at WI08 values. This is the SE fit in the third column quoted with errors determined from the corresponding diagonal elements of the covariance matrix. As a simpler point of comparison, a second SE fit has been done without allowing for renormalization of the fit (last column). Here the fit is significantly worse.

Starting from this last SE fit, and its best χ^2, we see from Eq. (4) that the χ^2 should increase quadratically as one moves away from the minimum. In Fig. 1(a), we compare the χ^2 variation for the two S-wave amplitudes as given by the corresponding error matrix and an actual fit to data (the other two partial waves are held at their best values $\hat{\delta}_{P11}$ and $\hat{\delta}_{P33}$). Shown is a region well beyond the $\Delta\chi^2 = 2.30$ ellipse that marks the 68% confidence region of a two-parameter fit (and well beyond the $\Delta\chi^2 = 4.72$ ellipse of a 4-parameter fit). The parabolic behavior of the correlated χ^2 predicts well the actual

TABLE I. Fits to data near $T_\pi = 90$ MeV. Quoted are the phase shifts $\hat{\delta}_i$ (deg). WI08 [2] is the energy-dependent (ED) fit; SE is the single-energy fit, allowing renormalization, based on the ED fit. The last column gives a SE fit without allowing renormalization of the fit (see text).

90 MeV SE (87–92) MeV	WI08 (ED)	WI08 (SE)	WI08 (SE-No Renorm)
S_{11}	8.43	8.11(0.11)	8.02(0.11)
S_{31}	−8.21	−8.11(0.10)	−7.68(0.10)
P_{11}	−1.01	−0.71(0.09)	−0.58(0.09)
P_{33}	17.31	17.16(0.05)	16.68(0.05)
χ^2/data	150/121	124/121	301/121

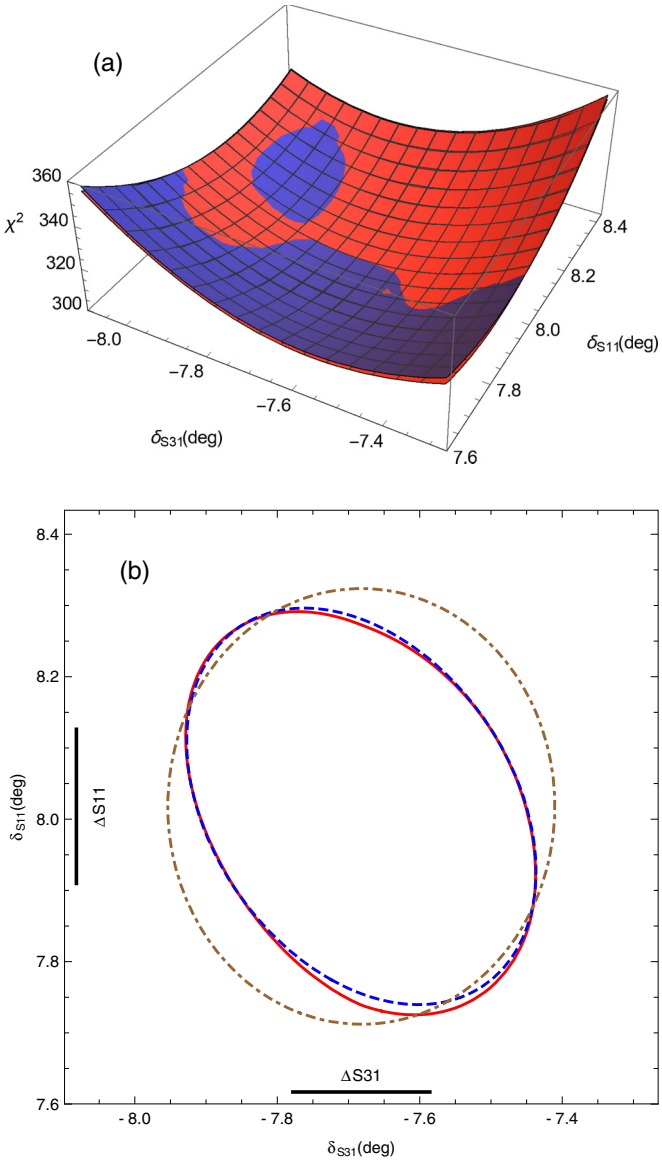

FIG. 1. The χ^2 without renormalization (last column of Table I). (a) The χ^2 of the SES for $T_\pi \in [87,92]$ MeV as a function of δ_{S11} and δ_{S31} with the values of all other partial waves fixed at the minimum. The red (blue) surface shows the actual χ^2 (the χ^2 predicted from the covariance matrix). (b) Contours of constant $\Delta\chi^2 = 8$ for the actual χ^2 (solid red), for the χ^2 predicted from the full covariance matrix (dashed blue), and from the covariance matrix neglecting correlations (dash-dotted brown line). Parameter errors $\Delta S11$, $\Delta S31$ are indicated with bars.

χ^2 within the shown region. Thus, the $\mathcal{O}(\mathbf{A}^3)$ corrections of Eq. (4) are indeed very small well beyond the region in which a fit can be considered good.

In Fig. 1(b) we show the $\Delta\chi^2(\hat{\Sigma}) = 8$ ellipse from $\hat{\Sigma}$ (solid, red) and compare with the actual $\Delta\chi^2 = 8$ line (dashed, blue). The figure shows again that the covariance matrix predicts the rise of the χ^2 well. For example, at $(\delta_{S11},\delta_{S31}) = (8.42 \text{ deg}, -7.28 \text{ deg})$ the difference between $\Delta\chi^2(\hat{\Sigma})$ and the actual $\Delta\chi^2$ is only 2, compared to an absolute scale given by $\chi^2 = 359$ at this point. Along the axes, the figure also shows the parameter errors, given by the maximal extensions of the $\Delta\chi^2 = 1$ ellipse.

In addition, a $\Delta\chi^2 = 8$ error ellipse is shown that is obtained from the covariance $\hat{\Sigma}_0$ in which all off-diagonal elements are set to zero, i.e., ignoring correlations (dash-dotted, brown). The effect is sizable: At $(\delta_{S11},\delta_{S31})$ considered before one has $\Delta\chi^2(\hat{\Sigma}) = 56$ and $\Delta\chi^2(\hat{\Sigma}_0) = 31$, i.e., only 55% of the correlated value. At higher energies, where parameters are generally more strongly correlated, this discrepancy becomes much larger.

The breakdown of χ^2 contributions is then as follows: the χ^2 at the minimum is $\chi^2(\hat{\mathbf{A}}) = 301$, the contribution from correlations amounts to $\Delta\chi^2 = 56$, and the sum $\chi^2 = 357$ is 0.5% different from the actual χ^2 found from a comparison to data. In contrast, if one had mistakenly regarded the SE solutions as uncorrelated data points (as done in some analyses), a meaningless $\chi^2 = 31$ would have been obtained at $(\delta_{S11},\delta_{S31}) = (8.42 \text{ deg}, -7.28 \text{ deg})$.

To conclude this section, the effects of normalization are discussed. Recall that the minimum at $\mathbf{A} = \hat{\mathbf{A}}$ in the standard SE fit (third column of Table I) is obtained allowing for renormalization of the minimizing function. The covariance matrix is then numerically estimated from the Hessian, $\hat{\Sigma} = 2H^{-1}$ with $H_{ij} = \partial^2\chi^2/(\partial A_i \partial A_j)$, using the penalized χ^2 from Eq. (1), i.e., including the renormalization. To that end, the covariance matrix includes information about the change in normalization when moving away from the minimum, but with a value frozen at the minimum. Moving away from the minimum, both the fitted amplitudes and the fit function normalization factors work to reduce the χ^2, resulting in a nonquadratic variation. However, if one is close to the minimum, the error matrix should still give a reasonable estimate of the data χ^2.

In Fig. 2(b), the $\Delta\chi^2$ curves from the normalizable SE solution (thick) lines are shown. The curves from the previously discussed case (no normalization) are replotted for comparison (thin lines). The thick solid red (thick dashed blue) lines show the actual $\Delta\chi^2$ values (the $\Delta\chi^2$ values predicted from the covariance matrix). We observe larger deviations of the actual χ^2 from the predicted one, which are a consequence of the discussed dynamic normalization, changing at any point in parameter space for the evaluation of the actual χ^2. Note, however, that this example has been chosen for the $\Delta\chi^2 = 8$ contour, i.e., far away from the minimum. There, a maximal deviation of actual and predicted χ^2 of 5% is observed.

For further illustration, Fig. 3 shows a selection of data from the considered $T_\pi = 87$–92 MeV energy bin and the SE fit obtained allowing normalization. The effect of normalization is visible for the differential cross section, which acquires a normalization factor of 0.98, constrained by the penalty term in Eq. (1). The factor, not applied in the figure, shifts the curve closer to the data, significantly reducing the χ^2.

A. Fits with fewer parameters

Some theory or model approaches describe fewer partial waves than provided in the covariance matrices. For example, chiral unitary approaches are often restricted to the lowest partial waves. How should one use the covariance matrices in these cases?

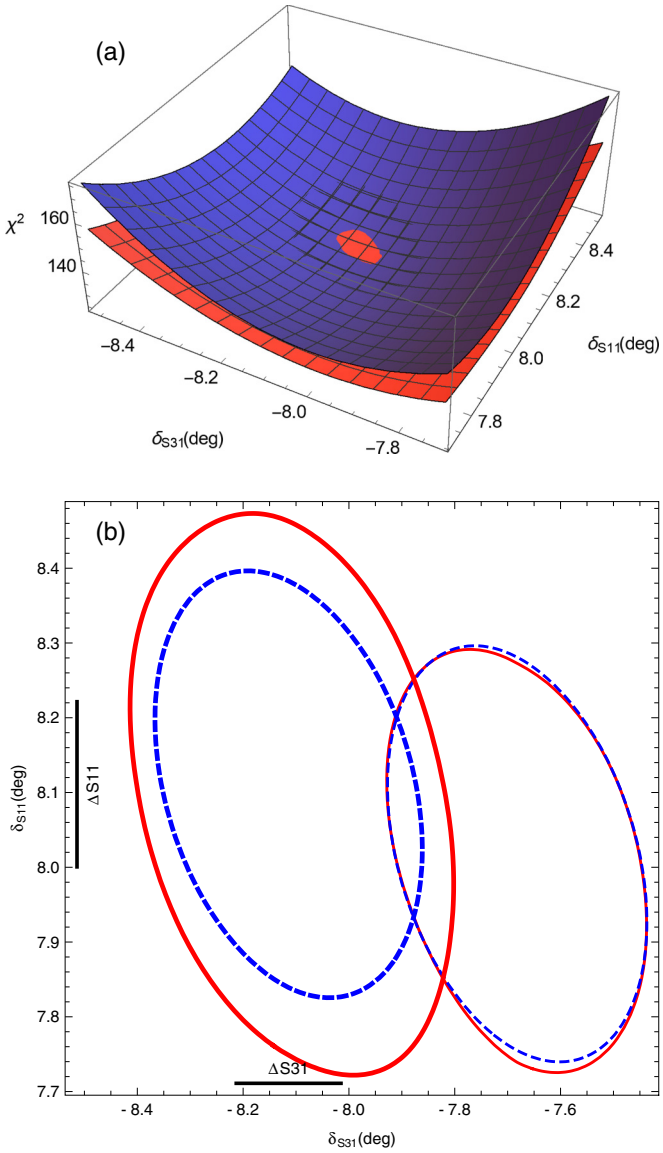

FIG. 2. The χ^2 with renormalization. Notation as in Fig. 1. (a) The red (blue) surface shows the actual χ^2 with renormalization (the χ^2 predicted from the covariance matrix). (b) Contours of constant $\Delta\chi^2 = 8$ for the actual χ^2 with renormalization (thick solid red), the χ^2 predicted from the covariance matrix (thick dashed blue), and the case without renormalization from Fig. 1 (thin lines).

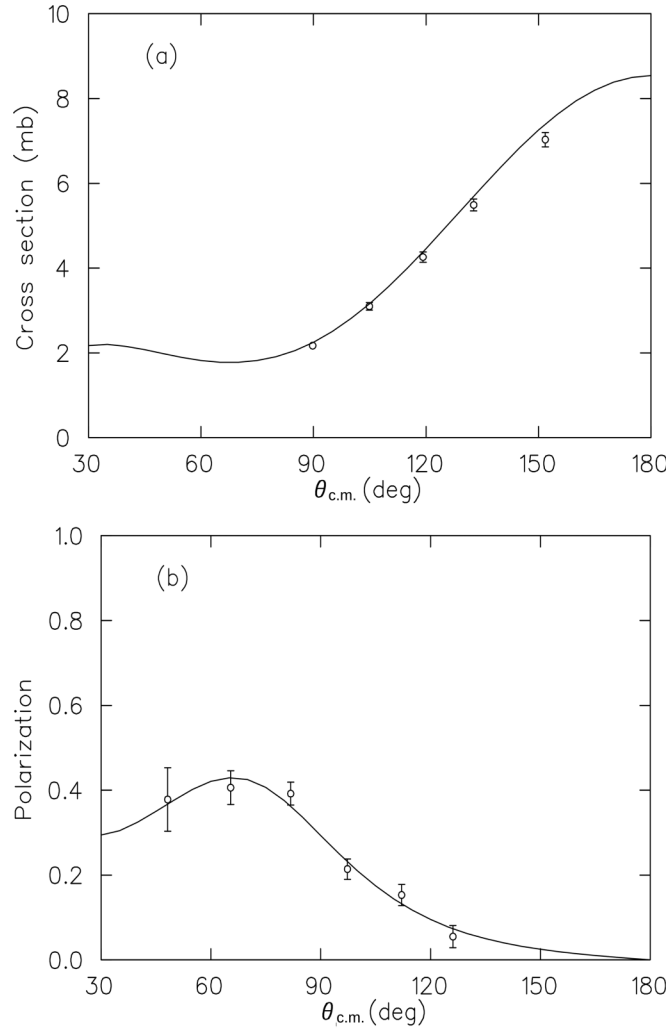

FIG. 3. (a) Differential cross section at $T_\pi = 91.7$ MeV and $\pi^+ p$ data of Ref. [67]. (b) Polarization (P) at $T_\pi = 87.2$ MeV and $\pi^+ p$ data of Ref. [68]. The 90 MeV SE fit is shown; the normalization N from Eq. (1) acquires a value of $N = 0.98$ for the differential cross section (not applied in figure).

As an example, assume that model M describes δ_{S11}, while the covariance matrix comprises δ_{S11} and δ_{S31} (see, e.g., the figures of this section). Suppose δ_{S11} in model M takes the value $\delta_{S11} = \hat{\delta}_{S11} + \Delta S11$. In the δ_{S11},δ_{S31} space, this corresponds to the right vertical tangent to the $\Delta\chi^2 = 1$ ellipse. Then, there exists one value δ_{S31} such that indeed $\Delta\chi^2 = 1$. On the other hand, by marginalizing the bivariate distribution over δ_{S31}, one obtains a normal distribution with variance $(\Delta S11)^2$, corresponding to a covariance matrix $\hat{\Sigma} = (\Delta S11)^2$. According to that reduced covariance matrix, the $\Delta\chi^2$ at $\delta_{S11} = \hat{\delta}_{S11} + \Delta S11$ has also increased by one, $\Delta\chi^2 = 1$. In summary, fitting the reduced covariance matrix is equivalent to fitting the entire covariance matrix, with δ_{S11} coming from model M, and optimizing all other parameters simultaneously. (Within M one cannot make any statement about the size of these other parameters or partial waves.)

The generalization to several parameters is straightforward. It can be shown that the reduced covariance matrix after marginalization is given by simply eliminating, from the full covariance matrix, the rows and columns corresponding to the marginalized parameters. Then, model M with fewer partial waves is fitted to that reduced matrix, and the unchanged $\chi^2(\hat{\mathbf{A}})$ is added according to Eq. (4).

V. SUMMARY AND CONCLUSIONS

Covariance matrices and other fit properties of the SAID SE solutions are provided to allow other groups to carry out correlated χ^2 fits to the elastic πN scattering reaction. In principle, the obtained χ^2 is then a good approximation to the χ^2 one would obtain if fitting directly to experimental data.

This has various practical advantages: Coulomb corrections are not an issue and normalization factors are included. However, the latter bear some subtleties as discussed. Furthermore, when fitting to SAID SE solutions, in the proposed manner, one implicitly accepts the chosen bin width and omission of nonlinear contributions to the χ^2 beyond the covariance matrix. In practice, we found these effects to be negligible, with the largest discrepancies coming from normalization. However, it has been checked that, close to the minimum, this effect is under control.

With correlated χ^2 fits, it is now possible to fit the SAID SE solutions in a statistically meaningful way. For baryon spectroscopy, this is a prerequisite to quantify the significance of resonance signals, usually performed in multireaction fits in which, so far, the precise statistical impact of πN partial waves has been unknown. Other approaches, such as quark-model calculations, CHPT, or unitary extensions thereof, can also benefit from the proposed fitting scheme, allowing, e.g., for an improved determination of low-energy constants. The numerical input needed to carry out correlated χ^2 fits is provided online.

ACKNOWLEDGMENTS

This work was supported in part by the U.S. Department of Energy Grant No. DE-SC0014133, by the National Science Foundation (CAREER Grant No. 1452055, PIF Grant No. 1415459), by GWU (startup grant), and by the DFG and NSFC through the Sino-German CRC 110. The authors gratefully acknowledge the computing time granted on the supercomputer JURECA at Jülich Supercomputing Centre (JSC, Forschungszentrum Jülich) and thank César Fernández Ramírez for useful discussions.

[1] K. A. Olive *et al.* (Particle Data Group), Chin. Phys. C **38**, 090001 (2014).
[2] R. L. Workman, R. A. Arndt, W. J. Briscoe, M. W. Paris, and I. I. Strakovsky, Phys. Rev. C **86**, 035202 (2012).
[3] R. A. Arndt, W. J. Briscoe, I. I. Strakovsky, and R. L. Workman, Phys. Rev. C **74**, 045205 (2006).
[4] R. A. Arndt, I. I. Strakovsky, R. L. Workman, and M. M. Pavan, Phys. Rev. C **52**, 2120 (1995).
[5] R. A. Arndt, W. J. Briscoe, I. I. Strakovsky, R. L. Workman, and M. M. Pavan, Phys. Rev. C **69**, 035213 (2004).
[6] G. Höhler, *Pion-Nucleon Scattering*, Landolt-Börnstein Vol. I/9b2 (Springer-Verlag, Berlin, 1983).
[7] R. L. Kelly and R. E. Cutkosky, Phys. Rev. D **20**, 2782 (1979).
[8] R. E. Cutkosky, R. E. Hendrick, J. W. Alcock, Y. A. Chao, R. G. Lipes, J. C. Sandusky, and R. L. Kelly, Phys. Rev. D **20**, 2804 (1979).
[9] R. E. Cutkosky, C. P. Forsyth, R. E. Hendrick, and R. L. Kelly, Phys. Rev. D **20**, 2839 (1979).
[10] D. Rönchen, M. Döring, H. Haberzettl, J. Haidenbauer, U.-G. Meißner, and K. Nakayama, Eur. Phys. J. A **51**, 70 (2015).
[11] D. Rönchen *et al.*, Eur. Phys. J. A **50**, 101 (2014); **51**, 63(E) (2015).
[12] H. Kamano, S. X. Nakamura, T.-S. H. Lee, and T. Sato, Phys. Rev. C **88**, 035209 (2013).
[13] D. Rönchen, M. Döring, F. Huang, H. Haberzettl, J. Haidenbauer, C. Hanhart, S. Krewald, U.-G. Meißner, and K. Nakayam, Eur. Phys. J. A **49**, 44 (2013).
[14] A. V. Anisovich, R. Beck, E. Klempt, V. A. Nikonov, A. V. Sarantsev, and U. Thoma, Eur. Phys. J. A **48**, 15 (2012).
[15] A. V. Anisovich, R. Beck, E. Klempt, V. A. Nikonov, A. V. Sarantsev, U. Thoma, and Y. Wunderlich, Eur. Phys. J. A **49**, 121 (2013).
[16] M. Shrestha and D. M. Manley, Phys. Rev. C **86**, 055203 (2012).
[17] M. Döring, C. Hanhart, F. Huang, S. Krewald, U.-G. Meißner, and D. Rönchen, Nucl. Phys. A **851**, 58 (2011).
[18] L. Tiator, S. S. Kamalov, S. Ceci, G. Y. Chen, D. Drechsel, A. Švarc, and S. N. Yang, Phys. Rev. C **82**, 055203 (2010).
[19] H. Kamano, S. X. Nakamura, T.-S. H. Lee, and T. Sato, Phys. Rev. C **81**, 065207 (2010).
[20] T. P. Vrana, S. A. Dytman, and T. S. H. Lee, Phys. Rept. **328**, 181 (2000).
[21] T. Feuster and U. Mosel, Phys. Rev. C **58**, 457 (1998).
[22] V. Shklyar, H. Lenske, and U. Mosel, Phys. Rev. C **72**, 015210 (2005).
[23] R. Arndt, W. Briscoe, M. W. Paris, I. Strakovsky, and R. L. Workman, Chin. Phys. C **33**, 1063 (2009).
[24] V. Bernard, N. Kaiser, J. Kambor, and U.-G. Meißner, Nucl. Phys. B **388**, 315 (1992).
[25] N. Fettes, U.-G. Meißner, and S. Steininger, Nucl. Phys. A **640**, 199 (1998).
[26] U.-G. Meißner and J. A. Oller, Nucl. Phys. A **673**, 311 (2000).
[27] N. Fettes and U.-G. Meißner, Nucl. Phys. A **676**, 311 (2000).
[28] N. Fettes and U.-G. Meißner, Nucl. Phys. A **679**, 629 (2001).
[29] T. Becher and H. Leutwyler, J. High Energy Phys. 06 (2001) 017.
[30] T. Fuchs, J. Gegelia, G. Japaridze, and S. Scherer, Phys. Rev. D **68**, 056005 (2003).
[31] M. Hoferichter, B. Kubis, and U.-G. Meißner, Nucl. Phys. A **833**, 18 (2010).
[32] A. Gasparyan and M. F. M. Lutz, Nucl. Phys. A **848**, 126 (2010).
[33] J. M. Alarcón, J. M. Camalich, and J. A. Oller, Phys. Rev. D **85**, 051503 (2012).
[34] J. M. Alarcón, J. M. Camalich, and J. A. Oller, Ann. Phys. **336**, 413 (2013).
[35] Y. H. Chen, D. L. Yao, and H. Q. Zheng, Phys. Rev. D **87**, 054019 (2013).
[36] M. Hoferichter, J. Ruiz de Elvira, B. Kubis, and U.-G. Meißner, Phys. Rev. Lett. **115**, 092301 (2015).
[37] M. Hoferichter, J. Ruiz de Elvira, B. Kubis, and U.-G. Meißner, Phys. Rev. Lett. **115**, 192301 (2015).
[38] M. Hoferichter, J. R. de Elvira, B. Kubis, and U.-G. Meißner, Phys. Rept. **625**, 1 (2016).
[39] K. A. Wendt, B. D. Carlsson, and A. Ekström, arXiv:1410.0646 [nucl-th] (unpublished).
[40] D. Siemens, V. Bernard, E. Epelbaum, A. Gasparyan, H. Krebs, and U.-G. Meißner, arXiv:1602.02640 (unpublished).
[41] P. C. Bruns, M. Mai, and U.-G. Meißner, Phys. Lett. B **697**, 254 (2011).
[42] M. Mai, P. C. Bruns, and U.-G. Meißner, Phys. Rev. D **86**, 094033 (2012).
[43] D. Ruić, M. Mai, and U.-G. Meißner, Phys. Lett. B **704**, 659 (2011).

[44] N. Kaiser, P. B. Siegel, and W. Weise, Phys. Lett. B **362**, 23 (1995).
[45] J. Nieves and E. R. Arriola, Phys. Rev. D **64**, 116008 (2001).
[46] T. Inoue, E. Oset, and M. J. Vicente Vacas, Phys. Rev. C **65**, 035204 (2002).
[47] D. Jido, M. Döring, and E. Oset, Phys. Rev. C **77**, 065207 (2008).
[48] M. Döring, E. Oset, and B. S. Zou, Phys. Rev. C **78**, 025207 (2008).
[49] M. Döring and K. Nakayama, Phys. Lett. B **683**, 145 (2010).
[50] M. Döring and K. Nakayama, Eur. Phys. J. A **43**, 83 (2010).
[51] M. Döring, M. Mai, and U.-G. Meißner, Phys. Lett. B **722**, 185 (2013).
[52] K. P. Khemchandani, A. Martínez Torres, H. Nagahiro, and A. Hosaka, Phys. Rev. D **88**, 114016 (2013).
[53] E. J. Garzón and E. Oset, Phys. Rev. C **91**, 025201 (2015).
[54] E. E. Kolomeitsev and M. F. M. Lutz, Phys. Lett. B **585**, 243 (2004).
[55] S. Sarkar, E. Oset, and M. J. Vicente Vacas, Nucl. Phys. A **750**, 294 (2005); **780**, 78(E) (2006).
[56] M. Döring, E. Oset, and D. Strottman, Phys. Rev. C **73**, 045209 (2006).
[57] M. Döring, Nucl. Phys. A **786**, 164 (2007).
[58] E. Oset and A. Ramos, Eur. Phys. J. A **44**, 445 (2010).
[59] A. Kiswandhi, S. Capstick, and S. Dytman, Phys. Rev. C **69**, 025205 (2004).
[60] C. S. An and B. Saghai, Phys. Rev. C **84**, 045204 (2011).
[61] B. Golli and S. Sirca, Eur. Phys. J. A **47**, 61 (2011).
[62] The SAID web site allows access to a variety of fits and the associated database. Results can be obtained from http://gwdac.phys.gwu.edu. The data needed to carry out correlated χ^2 fits described in this manuscript are made available through the πN branch of this site.
[63] The JPAC (Joint Physics Analysis Center) web site provides access to numerical results and formalism of a variety of hadronic reactions and decays. The results of this manuscript are accessed through http://www.indiana.edu/~jpac/CorrMatrixGWU.html.
[64] R. A. Arndt and M. H. MacGregor, Phys. Rev. **141**, 873 (1966). Here, the separation of parameter and normalization increments is demonstrated, assuming one is searching in the vicinity of the χ^2 minimum.
[65] G. D'Agostini, Nucl. Instrum. Meth. A **346**, 306 (1994).
[66] NNPDF Collaboration, R. D. Ball *et al.*, J. High Energy Phys. 05 (2010) 075.
[67] J. T. Brack *et al.*, Phys. Rev. C **34**, 1771 (1986).
[68] R. Meier *et al.*, Phys. Lett. B **588**, 155 (2004).